Cancer Cell Imaging and Photothermal Therapy in the Near-Infrared Region by Using Gold Nanorods

Xiaohua Huang,[†] Ivan H. El-Sayed,[‡] Wei Qian,[†] and Mostafa A. El-Sayed*,[†]

Contribution from the Laser Dynamics Laboratory, School of Chemistry and Biochemistry, Georgia Institute of Technology, Atlanta, Georgia 30332, and Otolaryngology—Head and Neck Surgery, Comprehensive Cancer Center, University of California at San Francisco, San Francisco, California 94143

Received October 24, 2005; E-mail: mostafa.el-sayed@chemistry.gatech.edu

Abstract: Due to strong electric fields at the surface, the absorption and scattering of electromagnetic radiation by noble metal nanoparticles are strongly enhanced. These unique properties provide the potential of designing novel optically active reagents for simultaneous molecular imaging and photothermal cancer therapy. It is desirable to use agents that are active in the near-infrared (NIR) region of the radiation spectrum to minimize the light extinction by intrinsic chromophores in native tissue. Gold nanorods with suitable aspect ratios (length divided by width) can absorb and scatter strongly in the NIR region (650−900 nm). In the present work, we provide an in vitro demonstration of gold nanorods as novel contrast agents for both molecular imaging and photothermal cancer therapy. Nanorods are synthesized and conjugated to anti-epidermal growth factor receptor (anti-EGFR) monoclonal antibodies and incubated in cell cultures with a nonmalignant epithelial cell line (HaCat) and two malignant oral epithelial cell lines (HOC 313 clone 8 and HSC 3). The anti-EGFR antibody-conjugated nanorods bind specifically to the surface of the malignant-type cells with a much higher affinity due to the overexpressed EGFR on the cytoplasmic membrane of the malignant cells. As a result of the strongly scattered red light from gold nanorods in dark field, observed using a laboratory microscope, the malignant cells are clearly visualized and diagnosed from the nonmalignant cells. It is found that, after exposure to continuous red laser at 800 nm, malignant cells require about half the laser energy to be photothermally destroyed than the nonmalignant cells. Thus, both efficient cancer cell diagnostics and selective photothermal therapy are realized at the same time.

I. Introduction

Reducing a material's size to the nanometer length scale (which is the length scale of the electronic motion that determines the material's properties) makes it sensitive to further reduction in size or a change in shape. In semiconductor nanoparticles, the property change results from quantum confinement of the electronic motion.[1] In metals, the properties of the surface become dominant and give nanoparticles new properties.[2] In noble metals, the coherent collective oscillation of electrons in the conduction band induces large surface electric fields which greatly enhance the radiative properties of gold and silver nanoparticles when they interact with resonant electromagnetic radiation.[3] This makes the absorption cross section of these nanoparticles orders of magnitude stronger than that of the most strongly absorbing molecules[4] and the light scattering cross section orders of magnitude more intense than that of organic dyes.[5] Thus, these particles act as excellent sensors and novel contrast agents for optical detection due to

their enhanced absorption and scattering, respectively. In addition, when it is realized that the strongly absorbed radiation is converted efficiently into heat on a picosecond time domain due to electron−phonon and phonon−phonon processes,[6] their potential use in photothermal therapy becomes obvious.

The use of nanoparticles in medicine is one of the important directions that nanotechnology is taking at this time. Their applications in drug delivery,[7−9] cancer cell diagnostics,[10−13] and therapeutics[14] have been active fields of research. The scattering properties of gold nanospheres have been used for cancer cell imaging using confocal microscopy[13,15] and simple

---

[†] Georgia Institute of Technology.
[‡] University of California at San Francisco.
(1) Alivisatos, A. P. *Science* **1996**, *271*, 933−937.
(2) Kreibig, U.; Vollmer, M. *Optical Properties of Metal Clusters*; New York: Springer, 1995.
(3) El-Sayed, M. A. *Acc. Chem. Res.* **2001**, *34*, 257−264.
(4) Link, S.; El-Sayed, M. A. *J. Phys. Chem. B* **1999**, *103*, 8410−8426.
(5) Yguerabide, J.; Yguerabide, E. E. *Anal. Biochem.* **1998**, *262*, 137−156.

(6) Link, S.; El-Sayed, M. A. *Int. Rev. Phys. Chem.* **2000**, *19*, 409−453.
(7) West, J. L.; Halas, N. J. *Annu. Rev. Biomed. Eng.* **2003**, *5*, 285−292.
(8) Paciotti, G. F.; Myer, L.; Weinreich, D.; Goia, D.; Pavel, N.; McLaughlin, R. E.; Tamarkin, L. *Drug Delivery* **2004**, *11*, 169−183.
(9) Jain, K. K. *Technol. Cancer Res. Treat.* **2005**, *4*, 407−416.
(10) Wu, X.; Liu, H.; Liu, J.; Haley, K. N.; Treadway, J. A.; Larson, J. P.; Ge, N.; Peale, F.; Bruchez, M. P. *Nat. Biotechnol.* **2003**, *21*, 41−46.
(11) Chan, W. C. W.; Maxwell, D. J.; Gao, X.; Bailey, R. E.; Han, M.; Nie, S. *Curr. Opin. Biotechnol.* **2002**, *13*, 40−46.
(12) Alivisatos, A. P. *Nat. Biotechnol.* **2004**, *22*, 47−52.
(13) Sokolov, K.; Aaron, J.; Hsu, B.; Nida, D.; Gillanwater, A.; Follen, M.; Macaulay, C.; Adler-Storthz, K.; Korgel, B.; Discour, M.; Pasquali, R.; Arap, W.; Lam, W.; Richartz-Kortum, R. *Technol. Cancer Res. Treat.* **2003**, *2*, 491−504.
(14) Hirsch, L. R.; Stafford, R. J.; Bankson, J. A.; Sershen, S. R.; Rivera, B.; Rrice, R. E.; Hazle, J. D.; Halas, N. J.; West, J. L. *Proc. Natl. Acad. Sci. U.S.A.* **2003**, *100*, 13549−13554.
(15) Sokolov, K.; Follen, M.; Aaron, J.; Pavlova, I.; Malpica, A.; Lotan, R.; Richartz-Kortum, R. *Cancer Res.* **2003**, *63*, 1999−2004.

dark-field microscopy.[16] Recently, photothermal therapy using the absorption properties of antibody-conjugated gold nanoshells[17] and solid gold nanospheres[18] has been demonstrated to selectively kill cancer cells, leaving the healthy cells unaffected.

To use long-wavelength laser irradiation that penetrates tissue for in vivo photothermal treatment (650−900 nm),[19] the absorption band of the nanoparticles has to be in the near-infrared (NIR) region. The absorption band of core−shell particles has been tuned by adjusting the ratio of the thickness of the gold shell to the diameter of the silica core (about 120 nm in diameter) and thus enables photothermal therapy in this region. Carbon nanotubes absorb naturally in this region and have recently been proposed as near-infrared therapy agents.[20] It is important to mention that surface plasmon field enhancement of the absorption of nanorods is predicted to be the strongest of all the different shapes of gold and silver nanoparticles.[21,22] By changing the shape of gold nanoparticles to gold nanorods, one can not only change the absorption and scattering wavelength from visible to the NIR region but also increase their absorption and scattering cross sections.

In the present work, we demonstrate the potential use of gold nanorods as a novel contrast reagent for dual molecular imaging using simple dark-field microscopy and selective photothermal therapy of cancer cells using a near-infrared low-energy continuous-wave (cw) laser. We have developed a synthetic method to enable the conjugation of the nanorods to anti-epidermal growth factor receptor (anti-EGFR) antibodies. Solid gold nanorods have several advantages over other photothermal contrast agents. The synthesis of gold nanorods with various aspect ratios, which enable tunable absorption wavelength in the NIR region[4,23−24] is quite simple and well-established. The appropriate size of the nanorods is quite small and is potentially useful in applications such as drug delivery and gene therapy. In addition, the biosafety of metallic gold is well-known and they have been used in vivo since the 1950s[25] and recently the noncytotoxicity of gold nanoparticles in human cells has been studied in detail by Wyatt et al.[26]

II. Experimental Section

A. Synthesis of Gold Nanorods. The nanorods were synthesized according to the seed-mediated growth method with some modifications.[27,28] Briefly, 0.0005 M auric acid (Sigma) in 0.2 M CTAB (cetyltrimethylammonium bromide, Sigma) was reduced at room temperature by cold sodium borohydride (0.01M) to yield small nanoparticles (less than 5 nm) as the seed solution. A 100 mL growth solution was prepared by reduction of 0.001 M auric acid in a solution containing 0.2 M CTAB, 0.15 M BDAC (Benzyldimethylhexadecylammonium chloride, Sigma) and 0.004 M silver salt with 70 μL of

0.0788 M ascorbic acid. 8μL of the seed solution was introduced into the growth solution and the nanorods were obtained after several hours. Higher yields of nanorods were obtained after a longer reaction time. Nanorods with various aspect ratios were obtained by changing the silver ion concentrations.

B. Preparation of Anti-EGFR/Au Nanorod Conjugates. The nanorods prepared above were capped with a bilayer of cetyltrimethylammonium bromide (CTAB), which is positively charged.[28] The original rods prepared in this way were centrifuged at 14 000 rpm twice to get rid of the extra free CTAB molecules in solution. The positively charged surface of the nanorods was changed to a negatively charged surface by exposing the nanoparticles to poly(styrenesulfonate) (PSS, MW = 18 000, Polysciences Inc.) polyelectrolyte solutions.[29] The extra PSS in solution was separated by centrifuging the rod solution at 8000 rpm, and the pellet was redispersed in *N*-(2-hydroxyethyl)piperazine-*N*′-2-ethanesulfonic acid (HEPES) solution (pH = 7.4). The PSS-capped nanorods were then mixed with antibody solution which was diluted in the same HEPES buffer and allowed to react for 20 min. The antibodies are probably bound to the PSS-coated nanorods by a mechanism similar to that used for binding antibodies to nanospheres,[15] i.e., by electrostatic physisorption interaction. The nanorods conjugated with anti-EGFR monoclonal antibodies were centrifuged and redispersed into phosphate-buffered saline (PBS; pH = 7.4) to form a stock solution with optical density around 0.5 at 800 nm. The anti-EGFR/nanorod conjugates were stable at 4 °C for several days.

C. Cell Culture and Cellular Incubation with Anti-EGFR/Au Nanorod. One nonmalignant epithelial cell line, HaCaT (human keratinocytes), and two malignant epithelial cell lines, HOC 313 clone 8 and HSC 3 (human oral squamous cell carcinoma), were cultured in Dulbecco's modification of Eagle's medium (DMEM, Cellgro) plus 5% fetal bovine serum (FBS, Gem Cell) at 37 °C under 5% CO$_2$. The cells were cleaved by trypsin and replated onto 18 mm glass coverslips in a 12-well tissue culture plate and were allowed to grow for 3 days. The coverslips were coated with collagen type I (Roche) in advance for optimum cell growth. The cell monolayer on the coverslips was taken out of the medium from the incubator, rinsed with PBS buffer, and then immersed into the anti-EGFR-conjugated nanorods solution for 30 min at room temperature. After the nanorods incubation, the cell monolayer was rinsed with PBS buffer, fixed with paraformaldehyde, coated with glycerol, and sealed with another coverslip.

D. Surface Plasmon Absorption and Light Scattering of Gold Nanorods on Cells. The light scattering images were recorded using an inverted Olympus IX70 microscope with a highly numerical dark-field condenser (U-DCW, 0.9−1.2), which delivers a very narrow beam of white light from a tungsten lamp on top of the sample. A 100×/ 1.35 oil Iris objective (UPLANAPO) was used to collect only the scattered light from the samples. The dark-field pictures were taken using an Olympus film camera with Kodak E100 VS film. The total extinction spectra of gold nanoparticles on single cells were measured using an SEE1100 microspectrometer under 20× magnification with a focus area of 8 μm in diameter. The scattered light from cells can be neglected due to the enhanced absorption and scattering from gold nanoparticles (by a factor of 10^5).

E. NIR Photothermal Therapy. For the laser irradiation experiment, a cw Ti:sapphire laser at 800 nm was used. This wavelength is in the NIR region at which the tissue has low absorption. It also overlaps efficiently with the longitudinal absorption band of the nanorods. The cell monolayer was immersed into the conjugated nanoparticle solution (OD$_{800\,nm}$ = 0.5) for 30 min, rinsed with PBS buffer, and then exposed to the red laser light at various power densities. The red laser at 800 nm was focused to a 1 mm diameter spot on the sample. Multiple regions on the slides were exposed to the laser light at different power densities for 4 min each and then stained with 0.4% trypan blue (Sigma) for 10 min to test cell viability. Dead cells accumulated the dye and

(16) El-Sayed, I. H.; Huang, X.; El-Sayed, M. A. *Nano Lett.* **2005**, *5*, 829−834.
(17) Loo, C.; Lowery, A.; Halas, N.; West, J.; Drezek, R. *Nano Lett.* **2005**, *5*, 709−711.
(18) El-Sayed, I. H.; Huang, X.; El-Sayed, M. A. *Cancer Lett.* **2005**, in press.
(19) Weissleder, R. *Nat. Biotechnol.* **2001**, *19*, 316−317.
(20) Shi Kam, N. W.; O'Connell, M.; Wisdom, J. A.; Dai, H. *Proc. Natl. Acad. Sci. U.S.A.* **2005**, *102*, 11600−11605.
(21) Hao, E.; Schatz, G. C. *J. Chem. Phys.* **2004**, *120*, 357−366.
(22) Hao, E.; Schatz, G. C.; Hupp, J. T. *J. Fluoresc.* **2004**, *14*, 331−341.
(23) Murphy, C. J.; Sau, T. K.; Gole, A. M.; Orendorff, C. J.; Gao, J.; Gou, L.; Hunyadi, S. E.; Li, T. *J. Phys. Chem. B* **2005**, *109*, 13857−13870.
(24) Kelly, K. L.; Coronado, E.; Zhao, L. L.; Schatz, G. C. *J. Phys. Chem. B* **2003**, *107*, 668−677.
(25) Sherman, A. I.; Ter-Pogossian, M. *Cancer* **1953**, *6*, 1238−1240.
(26) Connor, E. E.; Mwamuka, J.; Gole, A.; Murphy, C. J.; Wyatt, M. D. *Small* **2005**, *1*, 325−327.
(27) Murphy, C. J.; Jana, N. R. *Adv. Mater.* **2002**, *14*, 80−82.
(28) Nikoobakht, B.; El-Sayed, M. A. *Langmuir* **2001**, *17*, 6368−6374.

(29) Gittins, D. I.; Caruso, F. *J. Phys. Chem. B* **2001**, *105*, 6846−6852.
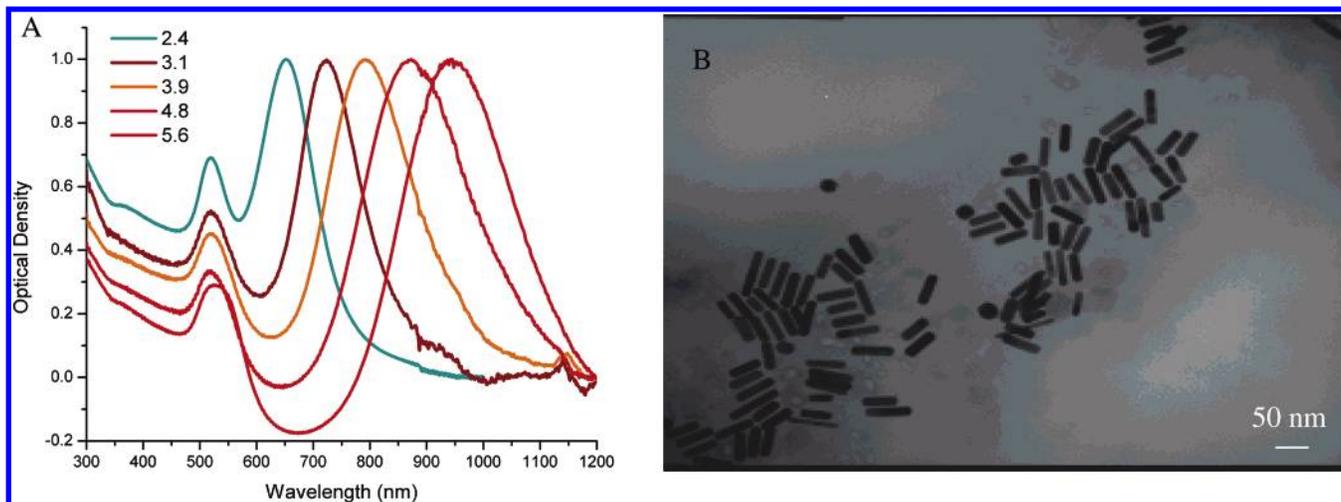
Figure 1. (A) Surface plasmon absorption spectra of gold nanorods of different aspect ratios, showing the sensitivity of the strong longitudinal band to the aspect ratios of the nanorods. (B) TEM image of nanorods of aspect ratio of 3.9, the absorption spectrum of which is shown as the orange curve in panel A.

were stained blue, while living cells eliminated it and remained clear. After staining, the samples were imaged under 10× in bright field.

III. Results and Discussion

A. Surface Plasmon Absorption and Light Scattering of Gold Nanorods on Cells. Gold nanospheres have one visible absorption band around 520 nm. The surface plasmon absorption of gold nanorods have two bands: a strong long-wavelength band due to the longitudinal oscillation of electrons and a weak short-wavelength band around 520 nm due to the transverse electronic oscillation. Figure 1A shows the observed optical absorption of gold nanorods of different aspect ratios obtained by varying the silver nitrate concentration during the growth process as described in the Experimental Section. The longitudinal absorption band shifts from the visible to the NIR region as the rod's aspect ratio increases. In this work, nanorods with an aspect ratio of 3.9 were chosen due to their absorption overlapping with a region of minimum extinction of the human tissues. The absorption band of the nanorods also overlaps the Ti:sapphire laser wavelength at 800 nm which we used in our laboratory. The transmission electron microscopy (TEM) image of the nanorods with an aspect ratio of 3.9 is shown in Figure 1B.

In dark-field microscopy, in which a narrow beam of white light is used at 100× magnification, different nanoparticles scatter different colored light, depending on their size and shape. For comparison, the light scattering images of anti-EGFR antibody-conjugated gold nanospheres (35 nm in diameter) after incubation with the cells[16] are also shown here in Figure 2A. Due to the fact that the surface plasmon oscillation frequency is in the visible region, both the enhanced absorption and scattered light are in the visible region. The nanospheres thus scatter green to yellow light. Figure 2B shows the light scattering images of anti-EGFR antibody-conjugated gold nanorods (aspect ratio of 3.9) after binding to the malignant and nonmalignant cells. The nanorods strongly scatter orange to red light due to their strong longitudinal surface plasmon oscillation with a frequency in the NIR region. Both anti-EGFR/Au nanosphere and nanorod conjugates bind specifically to the two types of malignant cells (right two columns) and give them a distinguishable imaging difference from the noncancerous cells. The

individual noncancerous cells are hardly identifiable due to the nonspecific interactions between the nanoparticles and the cells.

To quantify the bound nanoparticles on each cell type, the extinction spectra from single cells were measured using a micro-absorption spectrometer. Figure 2C shows the average extinction spectra of anti-EGFR/Au nanospheres on 20 different individual cells of each type, and Figure 2D shows the average extinction spectra of anti-EGFR/Au nanorods on 20 different individual cells of each type. In both nanosphere and nanorod cases, the gold concentration on the two types of malignant cells is over 2 times higher than that on the nonmalignant cells. This quantification does not necessarily correspond to the difference in the concentrations of EGFR between the malignant and nonmalignant cells because the nonmalignant cells might bind to some nanoparticles due to nonspecific interactions. Compared to the nanospheres, the amount of nanorods is much higher on both malignant and nonmalignant cells, mostly due to the interaction between PSS on the rod's surface and the proteins on the cell surface. Although the full extinction spectra of the nanorods were not completely recorded due to instrument cutoff at 1000 nm, it can be seen that the longitudinal extinction position is measured accurately and is red shifted compared with the extinction of free nanorods of the same size (see Figure 1A, orange curve). This red shift might be due to two factors. One is the change in the local refractive index on the nanoparticle surface caused by the specific binding of the anti-EGFR antibodies which bind to EGFR on the cell surface. The other is the interparticle interaction resulting from the assembly of nanoparticles on the cell surface. This interplasmon interaction of nanorods has also been observed on carbon nanotube surfaces and in solution.[30−32] The extinction of the gold nanorods onto the HaCat nonmalignant cells and the HSC and HOC malignant cells is too broad to give an accurate and useful value for the wavelength maxima for diagnostic purposes. This is unlike the results obtained on the binding to spheres, for which both the

(30) Correa-Duarte, M. A.; Pérez-Juste, J.; Sánchez-Iglesias, A.; Giersig, M.; Liz-Marzán, L. M. *Angew. Chem., Int. Ed.* **2005**, *44*, 4375−4378.
(31) Thomas, K. G.; Barazzouk, Said; Ipe, B. I.; Joseph, S. T. S.; Kamat, P. V. *J. Phys. Chem. B* **2004**, *108*, 13066−13068.
(32) Sudeep, P. K.; Joseph, S. T. S.; Thomas, K. G. *J. Am. Chem. Soc.* **2005**, *127*, 6516−6517.
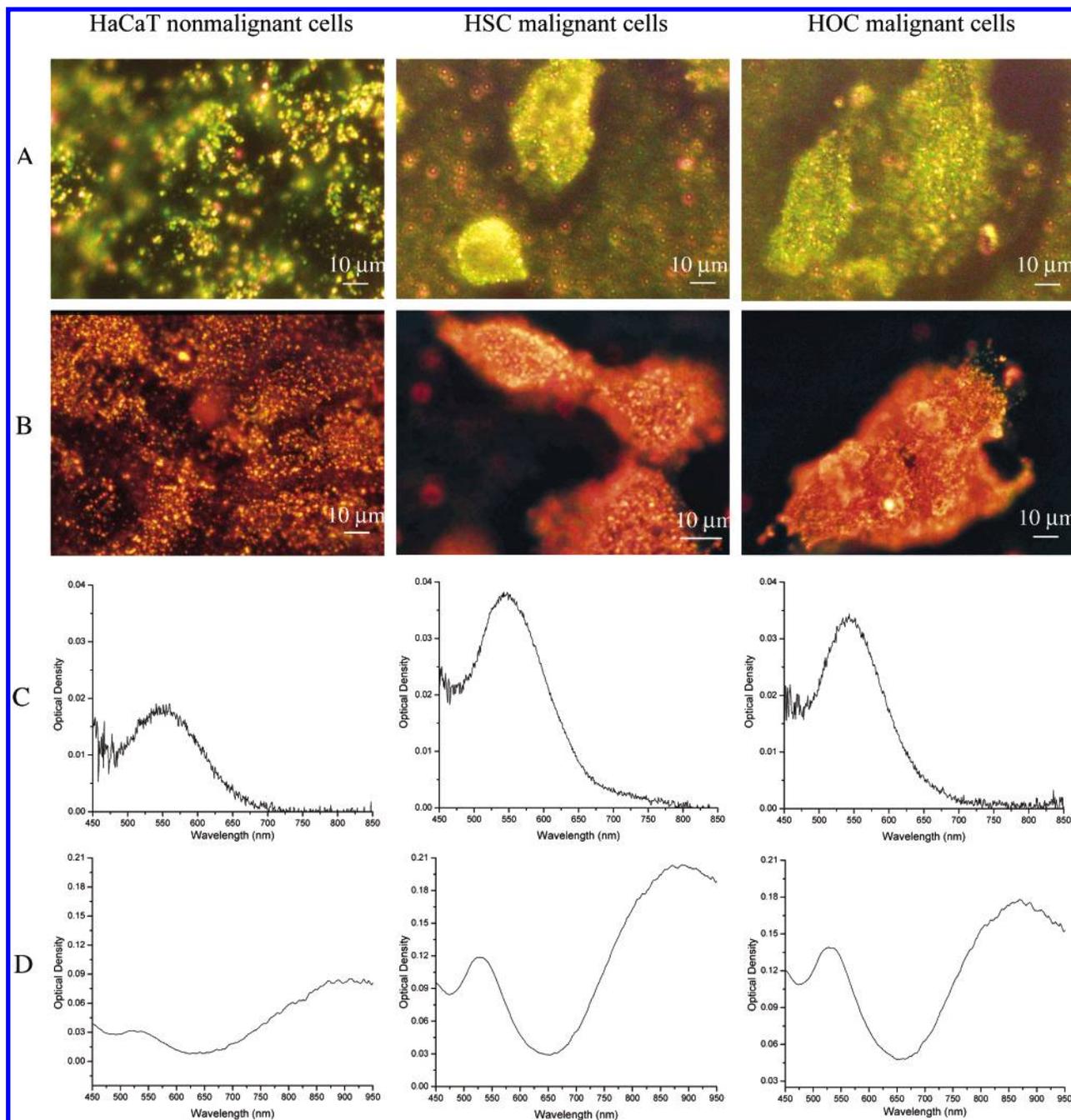
Figure 2. (A) Light scattering images of anti-EGFR/Au nanospheres after incubation with cells for 30 min at room temperature. (B) Light scattering images of anti-EGFR/Au nanorods after incubation with cells for 30 min at room temperature. (C) Average extinction spectra of anti-EGFR/Au nanospheres from 20 different single cells for each kind. (D) Average extinction spectra of anti-EGFR/Au nanorods from 20 different single cells for each kind. From gold nanospheres, the green to yellow color is most dominant, corresponding to the surface plasmonic enhancement of scattering light in the visible region, and from gold nanorods, the orange to red color is most dominant, corresponding to the surface plasmonic enhancement of the longitudinal oscillation in the near-infrared region.

bandwidth and band wavelength maxima are different for malignant and nonmalignant cells, affording a simple cancer diagnostic technique.[16]

B. Selective Photothermal Cancer Therapy Using Gold Nanorods. Our previous work demonstrated that antibody-conjugated gold nanospheres of 35 nm in diameter acted as efficient and selective photothermal absorbers for destroying cancer cells with a visible argon ion laser without affecting the surrounding nonmalignant cells.[18] The laser wavelength at 514 nm overlaps the surface plasmon absorption of the spherical nanoparticles, which has an absorption maximum at 520 nm.

By conjugation with anti-EGFR monoclonal antibodies that specifically target the molecular marker EGFR, the malignant cells can be destroyed with less than half the laser energy required to kill the normal cells due to the overexpresssion of the EGFR on the surface of malignant cells. However, at this wavelength, tissue penetration of the light is very low (less than 500 μm).[19] While this may be useful for superficial lesions, to treat cancer in vivo it is desirable to have deeper tissue penetration. The NIR region of the spectrum provides maximal penetration of light due to relatively lower scattering and absorption from the intrinsic tissue chromophores. In this region,
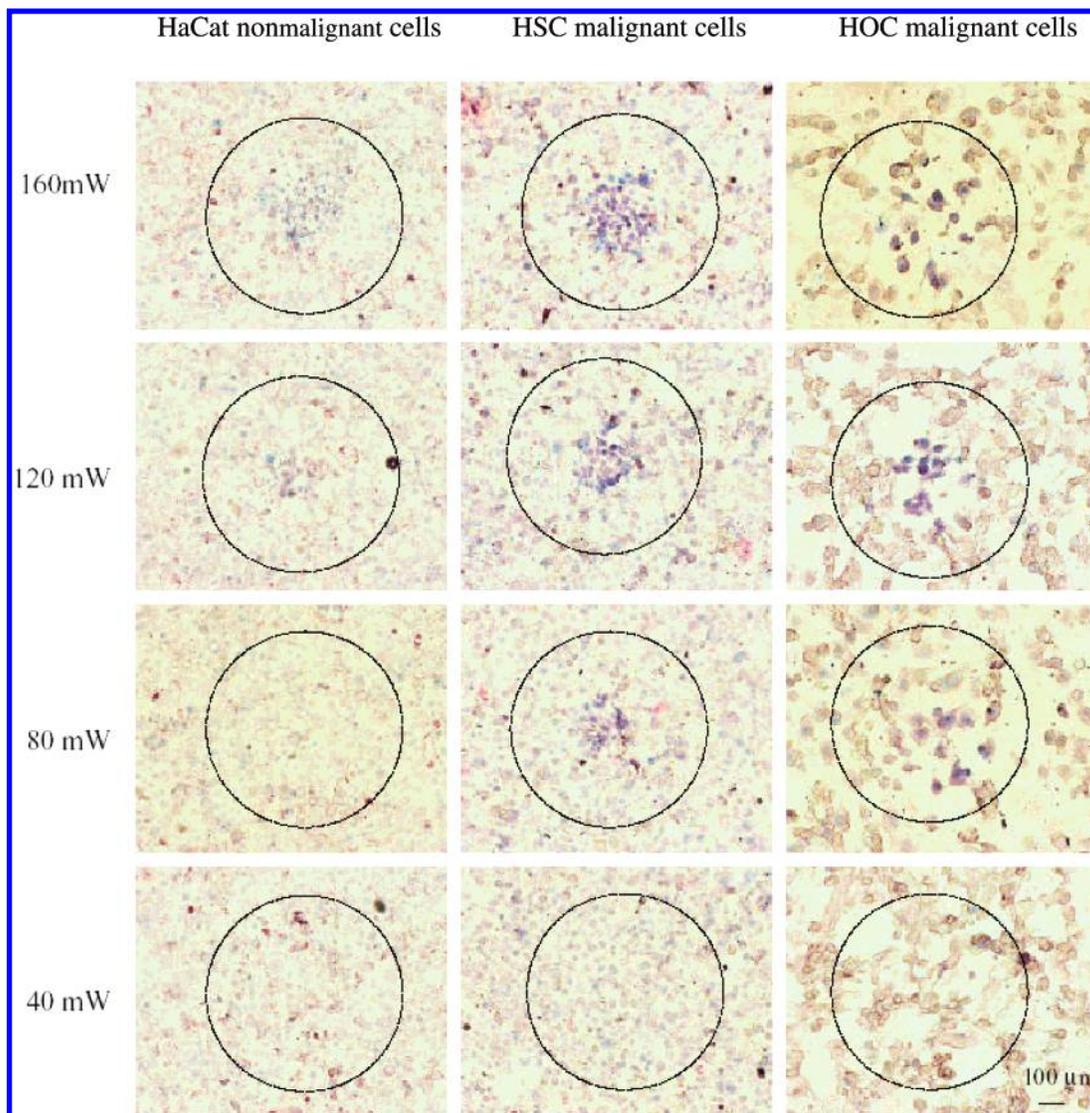
Figure 3. Selective photothermal therapy of cancer cells with anti-EGFR/Au nanorods incubated. The circles show the laser spots on the samples. At 80 mW (10 W/cm^2), the HSC and HOC malignant cells are obviously injured while the HaCat normal cells are not affected. The HaCat normal cells start to be injured at 120 mW (15 W/cm^2) and are obviously injured at 160 mW (20 W/cm^2).

the light penetration depth is up to 10 cm, depending on the tissue types.[19]

Since the absorption band of noble metallic nanoparticles is tunable by altering the nanoparticle shape or size, designing photothermal absorbing agents in the NIR region is possible. Other shapes of gold nanoparticles, such as branched,[33] pentagon,[34] and large prisms,[35] have the surface plasmon absorption in the NIR region. Nanorods are better candidates for this application due to the ability to accurately control the absorption maximum to the required wavelength by changing the aspect ratio, which can be realized by simply changing the silver ion concentration during the gold nanorod growth process. However, other properties, such as binding affinity of different nanoshapes and their capping molecules to the antibodies, should also be considered in the future.

After incubation with anti-EGFR antibody-conjugated gold nanorods for 30 min, cells are exposed to cw Ti:sapphire laser irradiation at power values of 40, 80, 120, 160, and 200 mW with a focus spot of 1 mm in diameter for 4 min each. The cells are then stained with trypan blue to test for their photothermal stability. Figure 3 shows images of samples irradiated at different laser energies.

Exposure to the red laser at 800 nm at and above 160 mW (20 W/cm^2) caused photodestruction of all HaCat normal cells, which is detected by the cell viability test with trypan blue (Figure 3, left column). Cell death is shown as a blue spot in a circular region that matches the laser spot size. The cells outside the laser spot are viable, as indicated by their ability to get rid of the trypan blue. This also indicates that the anti-EGFR/Au nanorods themselves are not cytotoxic. Reducing the laser energy to 120 mW decreases the proportion of blue cells in the laser spot. At this energy, only the laser spot center contains a sufficiently high energy density to cause cell destruction. The energy density at the edge of the laser spot is not high enough

(33) Hao, E.; Bailey, R. C.; Schatz, G. C.; Hupp, J. T.; Li, S. *Nano Lett.* **2004**, *4*, 327−330.
(34) Malikova, N.; Pastoriza-Santos, I.; Schierhorn, M.; Kotov, N. A.; Liz-Marzan, M. L. *Langmuir* **2002**, *18*, 3694−3697.
(35) Huang, W.; Qian, W.; El-Sayed, M. A. *Nano Lett.* **2004**, *4*, 1741−1747.

to cause cell injury, and thus the blue death cell spots become smaller than at higher energies.

Figure 3 (the middle column images) shows that the malignant HSC cells suffer photothermal injury at a lower laser power. Cell death occurs within the laser spots after exposure to the laser at and above 80 mW, which corresponds to 10 W/cm^2. The energy threshold for cell death of the HSC cells is about half that needed to cause cell death of the nonmalignant HaCaT cells. The dim blue color shown in the HSC cell images outside the laser spot is due to cells that died from prolonged exposure of the cells in buffer solution outside the cell incubator.

The HOC malignant cells also undergo photothermal destruction at and above 80 mW, while no cell death was observed at lower power (Figure 3, right column). The two malignant cells require about half the energy needed to kill the nonmalignant cells, which is due to the overexpression of EGFR on the cancer cells and the corresponding higher amount of anti-EGFR antibody-conjugated gold nanorods which absorb the light and convert it into heat at the cell surface. From the absorption spectra of the three types of cells in Figure 2, it can be seen that the amount of nanorods on the two malignant cells is over 2 times higher than that on the nonmalignant cells. The photothermally hot nanorods thus deliver more heat to the malignant cell membrane, leading to cell death at lower energy than that for the nonmalignant cells.

The above results suggest that nanorods conjugated to antibodies can be used as a selective and efficient photothermal agent for cancer cell therapy using a low-energy harmless near-infrared laser. Thus, for further in vivo applications, it is expected that the tumor tissue will be selectively destroyed at laser energies which will not harm the surrounding normal tissue due to the higher concentration of nanorods selectively bound to the tumor tissue. The threshold energy to kill the cancer cells in our work is found to be 10 W/cm^2, which is lower than that needed in the case of the core−shell particles.[14] This difference can result from a higher absorption cross section, a higher affinity constant for binding of the gold nanoparticles to the antibody, or a higher affinity constant for binding of the antibody to the cancer cell surface used.

It is known that many solid tumors, including brain, bladder, stomach, breast, lung, endometrium, cervix, vulva, ovary, esophagus, stomach, prostate, renal, pancreatic, glioblastoma, and squamous cell carcinoma cells, overexpress EGFR on the cell cytoplasm membrane to different degrees.[36] Targeting this specific molecule on the cell surface allows selective delivery of the nanorods with much higher concentrations to carcinoma cells and allows for selective photothermal therapy with a near-infrared laser for many types of cancer cells. The strong scattering of gold nanorods enables them to be imaging contrast agents as well. Thus, gold nanorods offer a new dual diagnostic imaging/therapy method in biomedical sensing and cancer therapy, tunable for use in the visible and NIR regions.

IV. Conclusions

This study demonstrates that gold nanorods are a novel class of optically active dual imaging/therapy agents due to their strong absorption and scattering of near-infrared light. By using surface plasmon resonant absorption spectroscopy and light scattering imaging, HSC and HOC malignant cells are easily distinguished from HaCaT nonmalignant cells due to the molecular targeting of overexpressed EGFR on the malignant cell surface. After exposure of these cells, incubated with anti-EGFR antibody-conjugated Au nanorods, to a near-infrared cw Ti:sapphire laser at 800 nm, different laser power energies were observed to cause photothermal destruction among malignant and nonmalignant cells. Increased uptake of the nanorods by the two malignant cells reduced the energy needed to cause destruction of these cells to about half of that required to cause death to the nonmalignant cells. Gold nanorods represent a biocompatible optically active absorber and scatterer that may potentially serve as the backbone for an assortment of designer compounds using a variety of vectors for molecularly targeted photodiagnostics and therapy.

JA057254A

(36) Herbst, R. S.; Shin, D. M. *Cancer* **2002**, *94*, 1593−1611.